

Diamond sources of the Juína region, Amazonian craton: textural and mineral chemical characteristics of Kimberley-type pyroclastic kimberlites

Izaac Cabral-Neto^{1,2}, Excelso Ruberti², D. Graham Pearson³, Yan Luo³, Rogério G. Azzone², Francisco V. Silveira¹, Vidyã V. Almeida¹

¹ Geological Survey of Brazil, Natal, Brazil, izaac.cabralneto@sgb.gov.br, vidya.almeida@sgb.gov.br, francisco.silveira@sgb.gov.br

² University of São Paulo, São Paulo, Brazil, exrubert@usp.br, rgazzone@usp.br

³ University of Alberta, Edmonton, Canada, gdpearso@ualberta.ca, ylo4@ualberta.ca

Introduction

Juína ranks as the second-largest diamond-producing municipality in Brazil, renowned worldwide for its remarkable sublithospheric diamond occurrences (e.g., Pearson et al. 2014) found in placer and kimberlite-hosted deposits. Despite this, the lack of petrological data on Juína's kimberlite pipes obstructs a comprehensive understanding of the nature and mantle source of these primary diamond sources. To address this gap, this study presents a textural and mineralogical analysis of representative kimberlite pipes in the Juína area, aiming to classify these rocks according to the updated kimberlite classification scheme proposed by Scott Smith et al. (2018). The findings help to refine our understanding of the primary diamond sources in Juína. A full report of the findings and the data can be found in Cabral-Neto et al. (2023).

Geological Setting

Juína is located in the southwestern Amazonian craton, within the Rio Negro-Juruena Province. The basement of this region comprises gneisses, granodiorites, tonalites, migmatites, granites, and amphibolites, with ages ranging from 1.8 to 1.5 Ga, intruded by anatectic granitoids (Tassinari and Macambira 1999). Locally, rocks from the Serra da Providência Intrusive Suite and the Parecis Basin predominate (Fig. 1).

Results

All pipes investigated petrographically (Aripuanã-2, Collier-1, -2, -4, Juína-1, and -5) consist of volcanoclastic kimberlite, showing pervasive alteration characterized by serpentine, clay minerals, and carbonate. They exhibit inequigranular, microcrystic textures, ranging from moderately to poorly sorted, mostly appearing loosely-packed and matrix-supported. These volcanoclastic rocks contain crustal and mantle xenoliths, magmaclasts, and macro- (>1 mm) and microcryst (≤ 1 mm) assemblages within a fine-grained siliciclastic or magmaclastic interclast matrix. Variations in colour, nature of the interstitial matrix, sedimentary structure, abundance and type of magmaclasts, as well as macro- and microcryst and xenolith presence, distinguish two textural types.

Spinel compositions exhibit wide variations, encompassing ranges in Al₂O₃ (2.1 - 40.9 wt%), Fe₂O₃ (below detection limit, bdl to 24.2 wt%), FeO (11.3 - 42.7 wt%), TiO₂ (bdl to 19.0 wt%), Cr₂O₃ (bdl to 52.7 wt%), and MgO (3.4 - 19.6 wt%). Most of Juína spinel compositions align within the "kimberlite" field, following the evolutionary trend of kimberlites (Trend 1) of Mitchell (1986) and Kjarsgaard et al (2022) (Fig. 2A).

The phlogopites demonstrate compositional similarities in TiO_2 and Al_2O_3 (wt%) with micas from kimberlite, although the fields overlap with orangeites and MARID (mica–amphibole–rutile–ilmenite–diopside) xenoliths. Mantle-derived pyrope garnets exhibit variable Cr_2O_3 concentrations ranging from bdl to 8.0 wt% (average 2.2 wt%), with 2.9 to 11.0 wt% CaO (average 5.1 wt%), bdl to 1.6 wt% TiO_2 (average 0.6 wt%), and bdl to 0.5 wt% MnO (average 0.2 wt%). The dominant garnet is low-Cr megacryst (G1), followed by lherzolitic (G9), high- TiO_2 peridotitic (G11), pyroxenitic (G4), and eclogitic (G3) garnets. No harzburgitic (G10) garnets were identified. In Zr versus Y space, most of the garnet analyses are indicative of “melt metasomatism” (Fig. 2B), and Zr/Hf versus Ti/Eu relationship suggests kimberlite-related metasomatism (indicated by values of Ti/Eu ratios between ~2500 - 7500 and Zr/Hf ratios between ~30-50; Shu and Brey 2015). Clinopyroxenes are Cr-rich (0.5 - 2.4 wt% Cr_2O_3) and have Mg# from 0.89 to 0.94. They show Zr concentrations ranging from 1 to 123 ppm (median = 22 ppm), La_N/Yb_N ratios ranging from 1 to 479 (median = 22.4), Ti/Eu ratios ranging from 136 to 7549 (median = 2755.4), Ca/Al ratios ranging from 6 to 259 (median = 14.6), and Zr/Hf ratios ranging from 12 to 46 (median = 27.6).

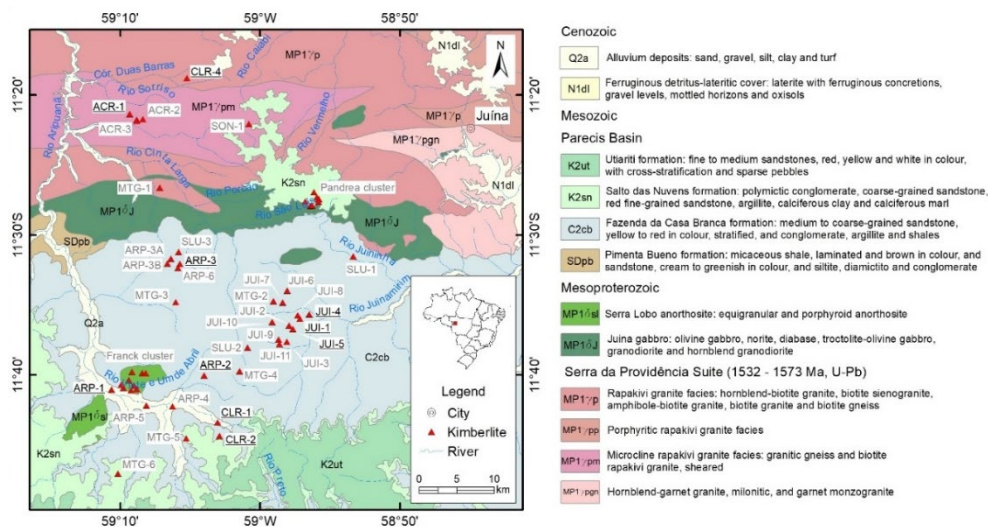


Figure 1: Simplified geological map of the Juína area with the location of the kimberlite bodies shown as red triangles. The bodies investigated in this study are labelled with bold black underlined names. Geology after Martins and Abdallah (2007) and kimberlite bodies after Nannini et al. (2017). ACR- Acuri; ARP- Aripuanã; CLR- Collier; JUI- Juína; MTG- Mato Grosso; SLU- São Luiz; SON- Sonho Alto

Discussion and Conclusions

Based on petrographic features and mineral compositions, we interpret the studied Juína pipes as archetypal kimberlites with pyroclastic emplacement styles filled with resedimented volcanoclastic kimberlite and Kimberley-type pyroclastic kimberlite variants. The composition and texture of the magmatic phases, particularly spinel and phlogopite, suggest crystallisation from kimberlite *sensu stricto* magmas. The presence of high-Na eclogitic garnets and the absence of high-Cr low-Ca G10 garnets within the mantle xenocryst suite suggest the likelihood of eclogitic diamonds among Juína’s lithospheric diamond populations. The Zr and Y contents, Ti/Eu and Zr/Hf ratios in the peridotite garnets, and Zr contents, Ca/Al, La_N/Yb_N (primitive-mantle normalised), Ti/Eu, and Zr/Hf ratios in the clinopyroxenes suggest a solid connection to kimberlite melt-related mantle metasomatism. Thermobarometry calculations indicate a relatively narrow stability window (825 - 936 °C and 32 - 36 kbar) for lithospheric diamonds in the Juína region. Our findings shed light on the primary sources of Juína’s diamonds and contribute to understanding the deep geological processes in the underlying lithospheric mantle beneath the Amazonian craton. The lack of depleted harzburgite garnets in the mantle sample indicate potential lherzolite/eclogite hosts for any lithospheric diamonds, while the location of the kimberlites in Paleo- to Mesoproterozoic basement

highlights a tectonic setting that is distinct from “classic” settings within Archean nuclei. Details for this case study are found on Cabral-Neto et al. (2023).

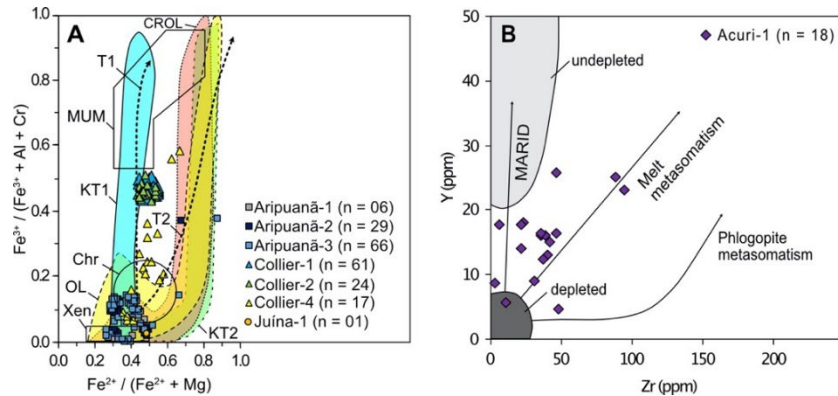


Figure 2: (A) $Fe^{3+}/(Fe^{3+} + Al + Cr)$ versus $Fe^{2+}/(Fe^{2+} + Mg)$ plot for spinels with trends of kimberlites (T1) and orangeites (T2) after Mitchell (1986), fields of xenocryst peridotite spinel (Xen), chromite (Chr) and magnesio-ulvöspinel-magnetite (MUM) after Roeder and Schulze (2008), and kimberlite Trend 1 (KT1), kimberlite Trend 2 (KT2), olivine lamproites (OL) and carbonate-rich olivine lamproites (CROL) after Kjarsgaard et al. (2022). (B) Y (ppm) versus Zr (ppm) plot for garnets from Acuri-1 with fields after Griffin et al. (1999) and Creighton et al. (2009).

Acknowledgements This research was supported by the Coordenação de Aperfeiçoamento de Pessoal de Nível Superior - Brasil (CAPES) - Finance Code 001, Fundação de Amparo à Pesquisa do Estado de São Paulo – FAPESP (2019/22084-8; 2023/11675-0), Brazilian National Research Council – CNPq (404020/2021-6, 310055/2021-0), Geological Survey of Brazil – SGB, and a Natural Sciences and Engineering Research Council of Canada – NSERC Discovery grant to Pearson.

References

- Cabral-Neto I, Ruberti E, Pearson DG et al (2023) Diamond sources of the Juína region, Amazonian craton: textural and mineral chemical characteristics of Kimberley-type pyroclastic kimb. *Min Petrol* 118:1-22.
- Creighton S, Stachel T, Matveev S et al (2009) Oxidation of the Kaapvaal lithospheric mantle driven by metasomatism. *Contrib Mineral Petrol* 157:491-504.
- Griffin WL, Shee SR, Ryan CG et al (1999) Harzburgite to lherzolite and back again: metasomatic processes in ultramafic xenoliths from the Wesselton kimberlite, Kimberley, South Africa. *Contrib Min Petrol* 134(2–3):232–250.
- Kjarsgaard BA, de Wit M, Heaman LM et al (2022) A Review of the Geology of Global Diamond Mines and Deposits. *Rev Mineral Geochem* 88(1):1–117.
- Martins EG, Abdallah S (2007) Geologia e Recursos Minerais da Folha Juína (SC.21-Y-C). CPRM.
- Mitchell R (1986) Kimberlites: mineralogy, geochemistry, and petrology. Plennun Press New York 442 p.
- Nannini F, Cabral-Neto I, Silveira FV et al (2017) Áreas kimberlíticas e diamantíferas do estado de Mato Grosso. CPRM.
- Pearson DG, Brenker FE, Nestola F et al (2014) Hydrous mantle transition zone indicated by ringwoodite included within diamond. *Nature* 507:221-224.
- Roeder PL, Schulze DJ (2008) Crystallization of groundmass spinel in kimberlite. *J Petrol*, 49(8):1473 1495
- Scott Smith BH, Nowicki TE, Russell JK et al (2018) A glossary of kimberlite and related terms. Scott-Smith Petrology Inc., North Vancouver, Part 1 – 144 pp, Part 2 – 59 pp, Part 3 – 56 pp.
- Shu Q, Brey GP (2015) Ancient mantle metasomatism recorded in subcalcic garnet xenocrysts: Temporal links between mantle metasomatism, diamond growth and crustal tectonomagmatism. *Earth Plan Sci Lett* 418:27–39.
- Tassinari CCG, Macambira MJB (1999) Geochronological provinces of the Amazonian Craton. *Epis-Newsmag Inter Union Geol Sci* 22(3):174–182.